Stormwater drainage for climate-resilient urban mobility

Xiaochi Shen* Wangyang Lai† Ming Lu‡

Abstract

Climate resilience requires cities to sustain essential functions as weather patterns change, but which infrastructure provides this capacity remains unclear. Combining 141,493 city-day observations from 99 Chinese cities with weather and infrastructure records, we show that stormwater drainage flattens the traffic–rainfall damage function. Rainfall above 24 mm raises travel time relative to free flow by 10.7 percentage points, whereas dedicated rainwater pipelines attenuate the marginal response by 20 percent at mean network density and 31 percent at one standard deviation above it. Mechanism tests point to surface-water removal rather than general infrastructure provision. Moving from inherited infrastructure to deliberate adaptation, China's Sponge City Program expanded rainwater-pipeline density and thereby flattened the traffic–rainfall gradient, demonstrating that public policy can build urban mobility resilience. Offsetting the projected increase in rainfall-induced congestion through mid-century would require 64,000 to 100,000 km of additional drainage pipelines across emissions scenarios, against a national stock of 310,000 km. The framework identifies both the infrastructure that weakens climate shocks and where additional capacity is most needed.

* Antai College of Economics and Management, Shanghai Jiao Tong University, China. Email: romanann@foxmail.com

† School of Advanced Agricultural Sciences, Peking University, China. Corresponding author, Email: laiwangyang@pku.edu.cn

‡ Antai College of Economics and Management, Shanghai Jiao Tong University, China. Email: luming1973@sjtu.edu.cn

Climate resilience is commonly assessed by whether cities can withstand acute shocks[1]. Yet resilience also depends on whether essential urban systems continue to function under recurrent weather shocks as the climate changes. Transport is central to this capacity: congestion reduces effective travel speeds, contracts accessible labor markets and imposes losses that increase with city size[2]. Precipitation repeatedly reduces effective road capacity, while climate change is altering the spatial distribution and intensity of rainfall[3].[1] Yet cities exposed to similar rainfall often experience markedly different traffic delays. This variation points to what climate-resilient infrastructure does: it weakens the link between a climatic hazard and the loss of an urban function.

Which investments provide this resilience is not obvious. Conventional transport policies, including congestion pricing, road expansion and public transport investment, principally target travel demand or transport capacity[7]. However, they do not directly restore the capacity lost when rainwater accumulates on roads. Potential candidates include stormwater drainage networks, permeable surfaces and urban green land. Dedicated rainwater pipelines convey runoff away from roads, while permeable and green surfaces reduce the volume entering the network. If these systems flatten the traffic–rainfall gradient, they should be understood not only as flood-control assets but also as infrastructure that preserves everyday urban mobility under climate stress.

We examine this proposition by linking 141,493 daily congestion observations from 99 Chinese cities between 2015 and 2019 to weather records and annual measures of drainage and other urban infrastructure. Day-to-day rainfall variation identifies the contemporaneous effect of precipitation on congestion, while its interaction with pipeline density reveals whether drainage flattens this response. We find that rainfall above 24 mm raises travel time relative to free flow by 10.7 percentage points, a burden that accumulates to roughly 359 million person-hours of additional commuting time a year across 289 cities. Dedicated rainwater pipelines attenuate the marginal response by approximately 20 percent at mean network density and 31 percent at one standard deviation above it. The attenuation is concentrated in stormwater-related infrastructure, operates through surface-water removal rather than visibility, and strengthens where terrain and urban form make runoff more difficult to manage.

Identifying drainage as a moderator, however, does not by itself show that resilience can be deliberately built. Existing pipeline density may reflect investments accumulated over decades and may be correlated with other city characteristics. China's Sponge City Program[8] offers an unusually informative setting: more than 60 percent of Chinese cities have experienced waterlogging in recent years[9], and the program allows us to move from studying resilience embedded in inherited infrastructure to deliberate adaptation. The results show that the Sponge City Program expanded pipeline density and flattened the traffic–rainfall gradient, demonstrating that urban mobility resilience can be built through targeted public investment.

Finally, we combine the estimated damage function with downscaled CMIP6 projections to

[1] Welfare losses in the United States are estimated at roughly $30 billion per year[4]; precipitation-driven commuting delays cost the African megacity Kinshasa alone more than $1.2 million a day[5]. Rainfall also damages urban functions beyond mobility, including respiratory health[6].

determine where future rainfall increases most exceed inherited drainage capacity. Offsetting the projected increase in rainfall-induced congestion through mid-century would require between 64,000 and 100,000 km of additional drainage pipelines depending on the emissions scenario, against a national stock of 310,000 km. Two features of that requirement run against intuition. The largest shortfalls arise not in the coastal cities where current losses are greatest, but across the North China Plain and the inland south, where rising rainfall meets only moderate legacy drainage. And the requirement is largest not under the highest-emissions pathway but under the most stringent mitigation one, because the rapid improvement in air quality that accompanies deep decarbonization lifts an aerosol suppression of monsoon rainfall[10].

The contribution is therefore both conceptual and operational. Climate risk is determined not only by future hazard exposure but also by the infrastructure that translates exposure into urban disruption. For rainfall-related mobility, stormwater drainage is one such system. More broadly, the framework offers a transferable investment principle: identify the infrastructure that flattens the relevant climate damage function, establish whether policy can expand it, and direct adaptation towards cities where projected hazards most exceed legacy capacity. The lesson for cities beyond China is not to replicate a particular pipeline standard, but to evaluate locally appropriate combinations of drainage networks, retention systems, permeable surfaces and green infrastructure according to their ability to preserve urban functions under a changing climate (Extended Data Fig. 1).

Results

Rainfall and congestion

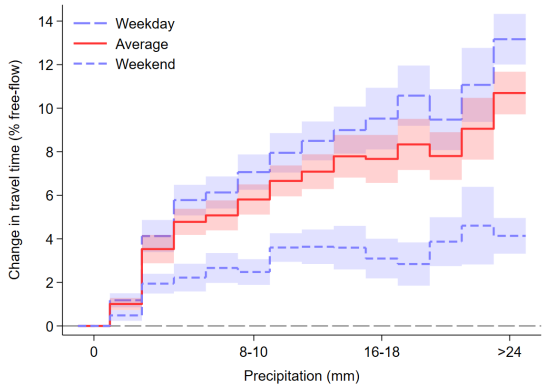
We begin with the hazard itself: how much travel time a day of rain costs, letting the effect differ across rainfall intensities. Rainfall has a large, nonlinear effect on urban traffic delays (Fig. 1a). Light precipitation (0–2 mm) raises travel time by about 1 percentage point relative to free flow, while heavy rainfall (>24 mm) raises it by 10.7 percentage points—more than 3 additional minutes on a typical 30-minute commute. In the linear specification, each millimeter of daily precipitation adds about 0.2 percent to travel time. Weekday effects exceed weekend effects by a factor of roughly three (Extended Data Table 1), consistent with the lower schedule flexibility of commuting travel[11]. The effect is also sharply contemporaneous: the day-of-rainfall coefficient is an order of magnitude larger than the coefficient on any preceding day, and leads beyond one day are indistinguishable from zero (Fig. 1b, Extended Data Table 2), a pattern that supports a causal reading, since day-to-day rainfall variation within a city and season is plausibly stochastic[12].

Applying these coefficients to each city's realized rainfall, its commuting population and its average car commute duration gives the annual burden (Methods, "Annual time losses"). Rainfall costs urban commuters in China about 359 million person-hours a year (95% CI 314 to 403 million), equivalent to some 179,000 full-time working years. The total covers the 289 cities with the required commuting and free-flow inputs, so it is a lower bound on the national loss. The loss

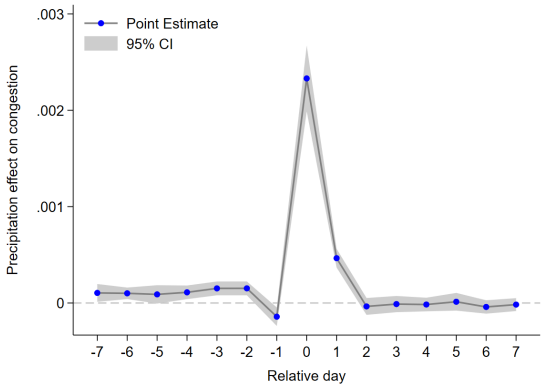
is heavily concentrated: the five largest losers account for a quarter of the national total and the top fifty for 58 percent (Fig. 1c), a concentration that follows the country's economic geography, with the Pearl River and Yangtze River deltas together bearing about 37 percent of the burden.

These estimates establish rainfall as a substantial and recurrent source of urban mobility loss. Yet rainfall exposure alone cannot explain why cities experiencing similar precipitation suffer markedly different delays. Climate resilience therefore depends not only on the magnitude of the weather shock, but also on the urban systems that translate that shock into service disruption. We next examine which urban infrastructure changes this translation by flattening the rainfall–congestion slope.

a Response by rainfall intensity



b Lead–lag structure



c Annual commuting time lost to rainfall, by city



Figure 1: Rainfall increases urban congestion, and the burden is spatially uneven. a, Estimated effects of precipitation on congestion by rainfall bin with 95% CI. Bins are 2 mm wide up to 24 mm, with a top bin above 24 mm; dry days are the omitted reference. **b,** Lead–lag analysis within a ± 7 day window. **c,** Annual commuting time lost to rainfall, by city, in person-hours, obtained by combining the estimated rainfall–congestion response with each city's commuting population and free-flow commute duration, on a round-trip basis, on the same weekday convention as the national totals reported in the text. The 98 cities of the estimation sample are shown together with 191 cities for which the damage function is extrapolated out of sample. Weather controls are temperature bins and wind speed (see Methods); fixed effects are city, date, and city-by-quarter. Standard errors clustered at city level.

Which infrastructure flattens the rainfall–congestion response

We now compare infrastructure types by how much each changes the rainfall–congestion relationship. The comparison covers surface and buried infrastructure, and among the buried networks it separates those that carry water from those that do not. Dedicated rainwater pipelines stand out. Cities with denser rainwater networks experience substantially smaller congestion responses to precipitation (Extended Data Table 3). At the city-level mean of 5.4 km/km^2, drainage absorbs approximately 20 percent of the rainfall effect. At one standard deviation above the mean (8.4 km/km^2), the attenuation reaches 31 percent—eliminating nearly a third of the travel-time penalty that rainfall would otherwise impose. Each city therefore has its own rainfall damage function: the travel time it loses per millimeter of rain, given its drainage.

The comparison across infrastructure types also sharpens identification. The principal threat to a drainage reading of this result is unobserved urban development: cities with dense drainage tend to be richer, better planned and better equipped in every other respect, so a flatter response might reflect general development rather than the pipes themselves. Urban networks, however, are largely built together, so that common component is shared across infrastructure types; entering them one at a time and then all at once therefore isolates what the rainwater network carries beyond it. Four lines of evidence indicate that the confound does not drive the result, and that the attenuation works through the physical removal of water from the road surface (Fig. 2).

First, among the four underground pipe networks—rainwater, sewage, water supply and gas—only rainwater pipelines retain a significant interaction when all four are entered in the same regression. Gas pipelines, buried infrastructure with no hydraulic role in stormwater removal, carry no detectable interaction when entered on their own, and when all four networks are entered together their coefficient differs sharply from that of the rainwater network ($p = 0.001$; Extended Data Table 3). Entered one at a time, the sewage and water-supply networks also carry a negative coefficient, which is what joint construction would produce: pipes of different kinds are laid together when a street is opened. Only the rainwater network survives their inclusion together.

Second, across a broader set of urban infrastructure types, Rainwater pipelines and green land coverage are the only measures that remain significantly negative when all infrastructure types are entered jointly (Extended Data Table 4). Bus and taxi fleets, road width and street lighting show no detectable buffering in either specification. General fiscal capacity would raise all of these together; instead the effect is confined to the two measures that move water rather than vehicles.

Third, the buffering acts on surface water rather than on visibility. Rainfall impedes traffic in two ways: water on the road and reduced visibility. Pipes remove the first and can do nothing about the second. Adding daily visibility to the specification attenuates the pipeline–precipitation coefficient by 3.6 percent, and adding its interaction with pipeline density by 4.1 percent; the pipeline–visibility interaction is close to zero ($p = 0.77$; Extended Data Table 5); and on standardized scales the pipeline response to precipitation is significantly larger than its response to reduced

visibility ($p = 0.020$).

Fourth, the buffering is strongest where runoff concentrates. Steep terrain funnels water into low-lying streets, and dispersed urban form lengthens the path water must travel before it reaches a drain; both raise the load a pipe network has to clear. In the flattest and most compact terciles of cities, pipelines provide no detectable attenuation, and the effect grows monotonically as terrain steepens and urban form disperses (Fig. 2c,d; Extended Data Table 6). A one-standard-deviation increase in terrain slope raises the average buffering by roughly 70 percent. Terrain slope is geologically given, ruling out reverse causality from drainage investment to the moderator. The two moderators are only weakly correlated ($r = 0.20$) and each shows the gradient when entered on its own; entered together, the urban-form gradient persists while the slope gradient attenuates.

Drainage capacity is therefore a moderator of rainfall-related congestion. But the networks measured here were laid over decades, and whether such capacity can be built within a policy horizon is a separate question. China's Sponge City Program provides a setting in which to ask it.

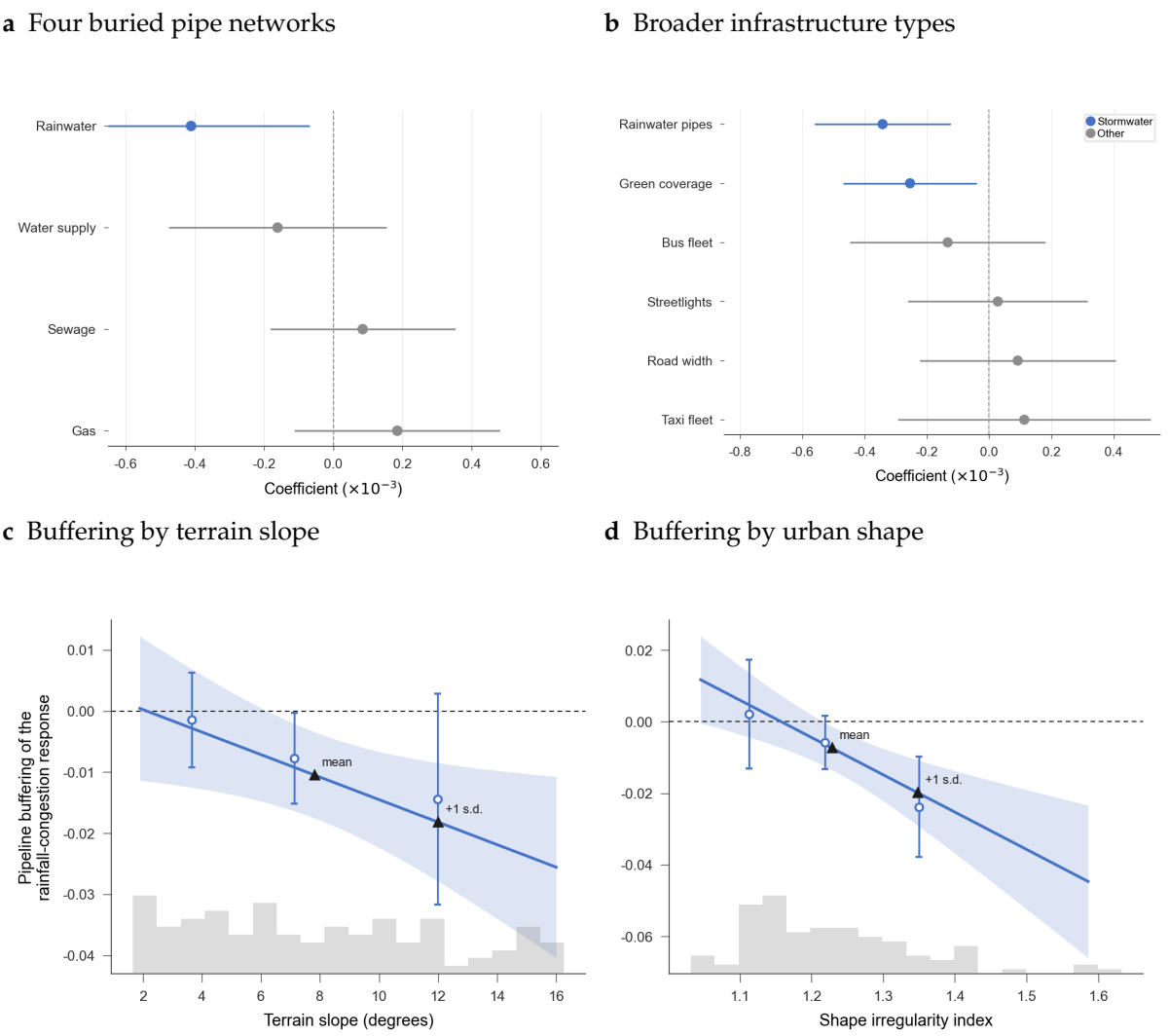


Figure 2: Drainage capacity flattens the rainfall–congestion slope, and does so where runoff concentrates. a, Buffering by each of the four buried pipe networks, entered together in a single regression. **b,** Buffering across broader infrastructure types, entered together in a separate regression, with stormwater-related measures in blue. Subway length is omitted because it is observed for a minority of cities (Extended Data Table 4). **c,d,** Marginal effect of pipeline density on the rainfall–congestion slope as a function of terrain slope (**c**) and urban shape irregularity (**d**), with 95% confidence bands from the delta method. Open circles are split-sample estimates by tercile; grey bars show the distribution of the moderator. Coefficients in **a** and **b** are interactions with rainfall, with each infrastructure measure standardized to unit variance.

Policy can move the rainfall–congestion gradient

If drainage shapes the rainfall damage function, then policies that expand drainage should flatten it. China's Sponge City Program provides a test. Announced around the end of 2015, it directs central transfers to thirty pilot cities, with the objective that 80 percent of built-up urban land absorb or reuse 70 percent of the rainfall falling on it by 2030[13], and it sets a target flood-protection level of a one-in-thirty-year storm against the one-in-one to one-in-five-year standard to which most Chinese drainage systems were built[8]. We date treatment from 2016 (Methods).

We ask first whether pilot cities differ at all in their sensitivity to rain, and only then what produced the difference. Pilot cities exhibit a flatter rainfall–congestion slope than non-pilots: each millimeter of precipitation raises travel time by about 0.1 percentage point less in pilot cities than in non-pilots (Extended Data Table 8, column 1). The congestion index is too short before treatment to test for parallel pre-trends, so we turn to the annual pipeline data, which run from 2011 to 2019.

Event-study estimates show that pilot designation was followed by a substantial expansion of rainwater pipeline density—approximately 1.25 km/km^2 relative to controls, from a baseline of 3.41 km/km^2—with no evidence of differential pre-trends (Fig. 3a,b). Sewer pipelines, water supply and urban green coverage show no significant response (Fig. 3c–f; Extended Data Table 7). The null for green coverage is notable: although green land attenuates the rainfall–congestion gradient in its own right (Extended Data Table 4), the program did not expand it—likely because underground pipelines can be installed beneath existing roads, whereas green infrastructure competes with development for scarce surface land.

Does the policy contrast run through the pipes? Adding the precipitation interactions of other infrastructure to equation (4) moves the policy interaction little: entered on its own, each group changes it by 9 to 13 percent. Pipeline density halves it and renders it insignificant (Extended Data Table 8). The lower rainfall sensitivity of pilot cities thus tracks how much drainage they have.

A pilot city's drainage has two parts. The pilots already had a denser network, and the program added 1.25 km/km^2. At the estimated buffering rate ($\rho = -1.17 \times 10^{-4}$), the addition alone flattens the slope by -1.47×10^{-4}, one-fifth of the pilot–non-pilot difference ($\theta = -7.25 \times 10^{-4}$); in time, it offsets about 6 percent of what rain costs a pilot city over a year, some 2.6 million person-hours across the pilot cities. Instrumenting the pipeline interaction with the program gives an estimate 1.7 times the OLS one and of the same sign, on a weak first stage (Extended Data Table 9).

Drainage capacity can therefore be changed at policy-relevant scale. Where to change it is a separate question, since the value of additional capacity depends on the rainfall a city will face and the network it already has.

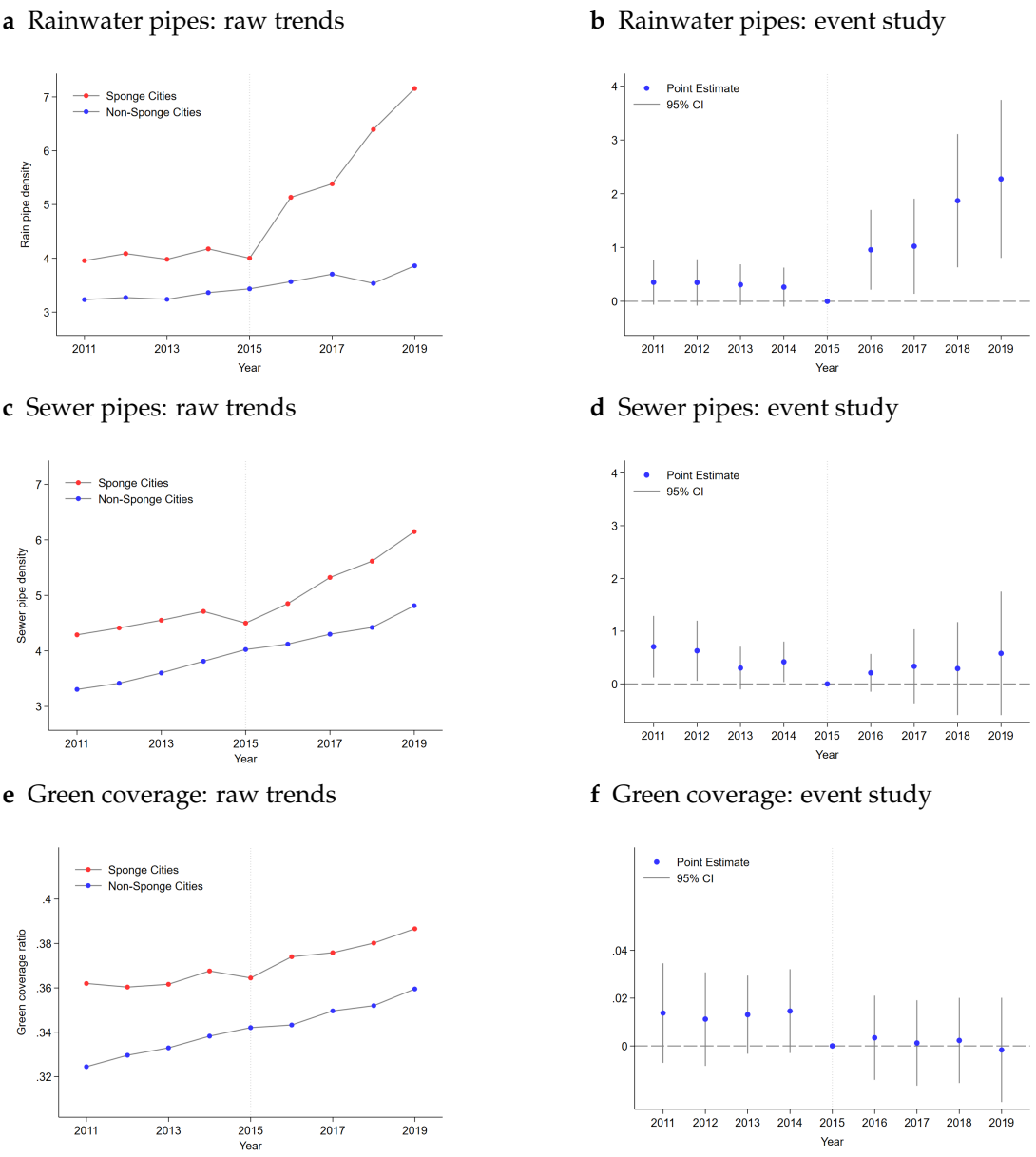


Figure 3: The Sponge City Program expanded rainwater drainage but not the other networks observed. Raw trends for pilot and non-pilot cities (left column) and event-study coefficients with 95% CI (right column); 2015 is the reference year and pilot cities are coded as treated from 2016. **a,b,** Rainwater pipeline density. **c,d,** Sewer pipeline density. **e,f,** Green land coverage. Rainwater and sewer pipeline density are in km/km^2; green land coverage is a share of built-up area.

Quantifying the adaptation gap under climate change

Climate change is redistributing the rainfall that cities have to handle: warming raises the frequency and intensity of extreme precipitation, with further increases over East and South Asia between 1.5 and 2°C of warming[3]. Adapting to that shift means sizing drainage against the rainfall a city will face rather than the rainfall it was built for, so we ask how much capacity each city would need under mid-century projections.

Drainage can be expanded, but not everywhere at once: pipes are costly to lay and cities compete for the same construction budgets, so capacity has to be directed where it buys the most. How much a city will need is set jointly by the rainfall it faces and the stock already in the ground, and the link between the two is the pair of coefficients estimated above: how much a millimeter of rain costs, and how much a kilometer of pipe absorbs. Combining them with projected precipitation gives the additional capacity each city would require to hold its congestion exposure constant—its drainage gap, measured as pipeline density and converted into kilometers of pipe by built-up area.

We take projected precipitation from three CMIP6 models under three emissions scenarios, spanning the range from stringent mitigation to none.[2] Rainfall rises by mid-century in most cities under all three, from 82 percent of our projection sample under SSP245 to 98 percent under SSP119; with drainage held at its 2019 level, each of those cities faces more rainfall-induced congestion than it does today. Aggregated across cities, the capacity that would offset the increase runs from roughly 64,000 km of pipeline under SSP585 to 100,000 km under SSP119, against a national stock of 310,000 km in 2019. Under SSP585 the median city needs 1.14 km/km^2 more (10th–90th percentile: 0.14 to 2.79). We report the gap as a measure of climate pressure in physical units rather than as an investment prescription.

Where that capacity is needed proves more stable across scenarios than how much of it. Under all three, the coastal cities that lose most time to rain today—those of the Pearl River and Yangtze River deltas—face comparatively small shortfalls, while the North China Plain faces large ones; what varies is how far the requirement reaches into the inland south, into provinces such as Guangxi and Guizhou (Fig. 4c–e). The two regions arrive at thin drainage by different routes: northern cities were built for a drier climate, whereas the inland south is wet but has not built to match. What they share is a mismatch between the rainfall they will face and the network already in place. The implication is counterintuitive: the cities paying most for rain today are among those best prepared for the rain to come, because the gap follows not rainfall itself but the distance between rainfall and what was built for it.

The scenarios themselves deliver a second surprise. The requirement is largest not under the highest-emissions pathway but under the most stringent mitigation one: 100,000 km under SSP119 against 68,000 km under SSP245 and 64,000 km under SSP585, falling on 282 cities rather than 275

[2]CMIP6 is the sixth phase of the Coupled Model Intercomparison Project, the coordinated set of global climate model experiments on which IPCC assessments draw. Shared Socioeconomic Pathways describe alternative futures for emissions and development: SSP119 assumes the most stringent mitigation, SSP245 an intermediate path, and SSP585 fossil-fueled growth with no effective mitigation.

(Fig. 4a). SSP119 stands apart because of the rainfall: the population-weighted increase in annual precipitation through mid-century is 10.0 percent under that scenario against 6.3 percent under SSP585 and 4.8 percent under SSP245. The two lower scenarios end up close together, since the requirement depends on the level of future rainfall as well as on its increase. What separates the scenarios over this horizon is aerosols rather than greenhouse gases: airborne particles suppress monsoon rainfall, and the pathway that cuts carbon emissions most deeply is also the one that cleans the air fastest, so lifting that suppression brings forward rainfall increases that greenhouse-gas forcing alone would deliver later[10]. We return below to what this implies for planning.

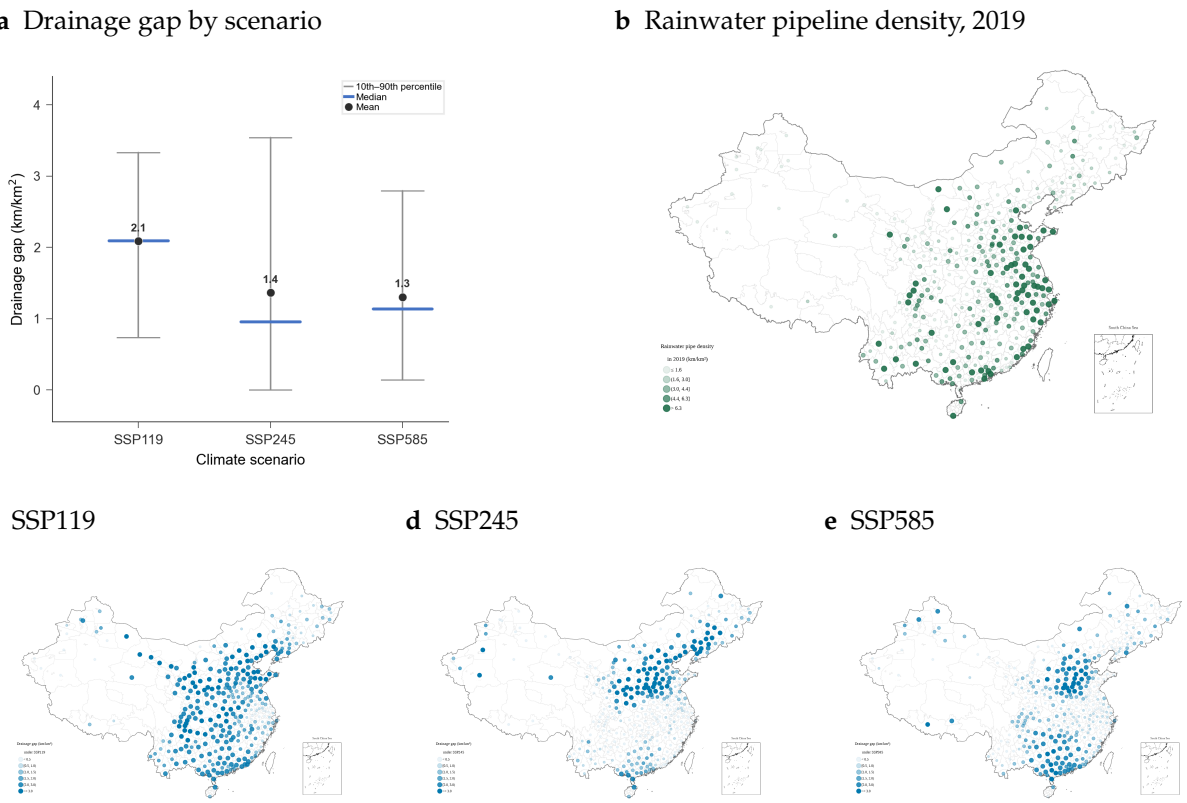


Figure 4: Adaptation needs are set jointly by shifting rainfall and legacy drainage, and do not disappear under strong mitigation. a, Distribution across cities of the additional pipeline density (km/km^2) required to hold congestion exposure at its 2021–2030 level through 2041–2050, under each of three emissions scenarios: mean (point, labeled), median (horizontal line) and 10th–90th percentile range (whiskers). **b,** Existing rainwater pipeline density (km/km^2) in 2019. **c–e,** Drainage gap by city under SSP119 (**c**), SSP245 (**d**) and SSP585 (**e**), on a common color scale. Cities whose projected rainfall does not rise are excluded (Methods). Projections use OLS estimates, with rainfall changes differenced within each climate model (see Methods).

Discussion

These findings reframe the relationship between weather and urban life. The congestion cost of rainfall is not fixed by climate but depends on the drainage a city has built underground, and can therefore be changed by investment. The shock is ordinary rain rather than catastrophic flooding, and the lever is not the transport network but the pipes that clear water from the road surface. What makes this reading hydraulic rather than a by-product of urban development is that the attenuation is confined to the networks that carry water, acts on rainfall but not on visibility, and grows with the terrain and urban form that concentrate runoff. On this evidence, everyday climate resilience is built underground. The Sponge City Program shows that this capacity is not merely inherited: pilot designation raised rainwater pipeline density, and the flatter rainfall–congestion slope of pilot cities is accounted for by the pipes rather than by anything else the program brought. Resilience of this kind can therefore be built within a policy horizon. Projecting the same damage function forward locates where it should be built, and the answer follows the distance between future rainfall and the network already in the ground rather than rainfall alone.

Related research has focused on climate disasters instead: the exposure of transport assets to flooding[14, 15], which grows as settlement expands into flood zones[16, 17], the recovery of mobility after extreme rainfall[18, 19], and the damage left once protection is built[20, 21]. Yet much of what a changing climate costs cities arrives as small losses, repeated often enough to accumulate. This everyday exposure poses a different question: not what damage survives protection, but what capacity keeps damage from rising. Answering it connects two strands of research that have developed apart. Transport economics has priced congestion[4, 22] and evaluated the instruments against it, from pricing to road capacity to transit[7], all of which act on travel demand or on capacity in normal conditions and none on the capacity that rain removes; the nearest work describes how travelers respond to weather and to transit availability[11, 23, 24], reallocating a disruption rather than shrinking it. Research on water infrastructure has valued these networks through health[25–27], flood protection[28–30] and urbanization[31], without following the pipes into everyday mobility. Drainage falls between the two: the water literature values it for purposes other than mobility, and the transport literature does not count it as a policy instrument at all. It also supplies one mechanism behind rainfall's measured effects on output[32, 33], part of which runs through the congestion drainage attenuates.

The comparison across infrastructure types also refines how infrastructure returns should be stated. Road and transit investments are evaluated by how much they raise travel speed or reduce delay under ordinary conditions. In Indian cities, a denser network of major roads raises speed mainly through its uncongested component, with an elasticity of about 0.08[22]; in Beijing, new subway lines cut the city's traffic congestion index by 0.728 units within 60 days of opening, a 15 percent reduction in delay[34].[3] Both capture the direct role of capacity-enhancing infrastructure

[3]The Beijing index is a 0–10 scale whose bands are defined by travel time relative to free flow, so it converts to the index used here: one unit corresponds to roughly 0.12–0.15 on our scale, and the 0.728-unit reduction to about 0.09–0.11. The conversion is approximate and is used only to place effect sizes side by side.

in alleviating congestion by reshaping modal choices and increasing throughput. On a common scale, a single day of heavy rainfall imposes a travel-time penalty of about the same size as a new subway line removes, with the opposite sign. Drainage is what limits that penalty, and it does so without touching normal-condition capacity at all. These are different objects—one shifts the level of congestion, the other flattens its response to a shock—and a city choosing between them is not choosing between two estimates of the same quantity. The broader implication is that climate-resilience investment should be evaluated by whether it flattens a damage function, not simply by how much capacity is added. On that criterion, the infrastructure that matters for rainfall and mobility is the infrastructure that moves water.

Three implications for policy follow. The first concerns how much drainage to build and where. On the evidence here, the answer is set by two quantities a city can observe—the rainfall it expects and the network it already has—combined with the parameters estimated above. It will differ from a ranking by rainfall alone: the greatest needs arise where rising precipitation meets a thin legacy network, not where precipitation is highest. The same logic has been shown to reorder transport investment itself: accounting for projected sea level rise changes not only the estimated returns to road upgrades but which routes should be built[35]. Terrain and urban form further modify the calculation, because the same expansion buys more attenuation where runoff concentrates. Design standards are the instrument through which such a calculation is normally implemented, and they lag: New York sized its drainage network for a three-year storm before the 1970s and a five-year storm after[36]. Risk assessments built on hazard intensity alone do not capture this dependence on what is already in the ground. To the extent that the cities facing the largest shortfalls also have the least fiscal capacity—a question we do not test—adaptation on this margin raises questions of spatial equity and intergovernmental transfers.

The second concerns the form that expansion takes. Rainwater pipelines and green land coverage both flatten the rainfall–congestion gradient, yet the Sponge City Program expanded only the former: underground pipelines can be laid beneath existing roads, whereas green infrastructure competes with development for land whose value is precisely what makes dense cities dense. For rapidly urbanizing countries adopting sponge-city-style programs, this suggests that adaptation will tend to run through grey infrastructure wherever land is scarce and expensive, whatever the stated preference for nature-based approaches. That tendency is worth designing around rather than assuming away, since the same development that seals permeable ground also raises the load the pipes must clear: simulations for European cities imply that each additional percentage point of impervious surface raises pluvial flood risk by 0.5–3.7 percent[37]. The two also differ in where they bind. Across 138 capital cities, drainage networks dominate flood reduction under ten-year rainfall while green space dominates under hundred-year rainfall[38]. Most of our observations are ordinary rainfall days rather than extremes, so the drainage margin identified here is the one that governs everyday exposure. The same trade-off arises wherever rainfall is rising: a city either adds capacity or absorbs the loss in travel time, and which side it falls on is set by the distance between its projected rainfall and its legacy network rather than by rainfall alone. Countries fac-

ing the sharpest precipitation changes therefore face the largest version of that choice, though the magnitudes depend on damage functions that would have to be estimated locally.

The third concerns which future to plan against. It is common to assess adaptation needs under the highest-emissions scenario, on the reasoning that doing so bounds the problem. At a mid-century horizon that reasoning does not hold. The aerosol effect behind our projections is a transitional one: across Asia and East Asia the median precipitation increase through the 2040s is largest under the most stringent mitigation scenario despite its far lower greenhouse-gas forcing, and only later in the century do greenhouse gases come to order the scenarios in the expected direction[10]. The drainage requirement inherits the mid-century ordering: on the three models available here it is some 57 percent larger under SSP119 than under SSP585, and falls on a wider set of cities. Adaptation planning should therefore be carried out over a scenario set that includes the stringent mitigation pathways, and near-term infrastructure requirements should be sized against the aerosol-driven rainfall increases those pathways bring forward, rather than against a single high-emissions upper bound.

Methods

Data

Congestion data. We use the daily Congestion Delay Index from Amap (Gaode), defined as the ratio of actual to free-flow travel time, which covers 99 major cities from October 2015 to December 2019. These cities are among the largest in the country and span every province. The index equals one when traffic moves at free-flow speed, so a coefficient of 0.01 means travel time rises by 1 percent of the free-flow duration. Effects in minutes are obtained as $\Delta T = \Delta\text{CDI} \times T^{\text{ff}}$, where T^{ff} is the city's free-flow one-way commute duration. We compute T^{ff} as the mean commute time in the 2015 one-percent population survey—a nationally representative household survey conducted midway between decennial censuses—divided by the city's mean index in 2015; for Beijing $T^{\text{ff}} \approx 27$ minutes. Because the index is normalized by each city's own free-flow time, a given index change corresponds to different absolute delays across cities.

Weather and climate data. Two distinct sources are used, and they serve different purposes. First, all estimation uses *observed* daily weather—precipitation, temperature, wind speed and horizontal visibility—from the Global Surface Summary of the Day (GSOD), with each city matched to its nearest station. Precipitation, temperature and wind speed are complete in the baseline estimation sample; visibility has additional missingness, reducing the usable sample to 133,778 city-days. Second, all *projected* rainfall, used only in the final section, comes from a separate gridded product: monthly precipitation for 2021–2050 from three CMIP6 models (EC-Earth3, GFDL-ESM4, MRI-ESM2-0) downscaled to 1-km resolution (0.0083333°) under SSP119, SSP245 and SSP585, taken from the dataset of Peng[39], with the delta downscaling procedure described in Peng et al.[40]. Precipitation there is stored in units of 0.1 mm per month. No projected quantity enters any regression.

Infrastructure data. Annual statistics for infrastructure are from the China Urban Construction Statistical Yearbook (2011–2019). The yearbook records rainwater, sewage, water-supply and gas pipelines separately. Pipeline density is defined as total rainwater pipeline length (km) divided by built-up area (km^2), the same definition applies to the other three networks, with numerator and denominator taken from the same yearbook year; yearbook figures are year-end stocks, and the interaction regressions assign each city-day the pipeline density of the corresponding calendar year. The same yearbook supplies the other infrastructure measures used in the comparison: green land coverage as a share of built-up area, bus and taxi fleets per capita, average road width, and streetlight density. Subway route length is observed only for the cities that had a system in operation, so it enters the comparison on a reduced sample.

Geographic data. Terrain slope is computed from the Shuttle Radar Topography Mission (SRTM) 90-m digital elevation model[41], averaged to the city level within administrative boundaries. Urban shape irregularity is measured on the continuous built-up area of each city as the mean distance between two points drawn at random within it, divided by the same quantity for a circle of equal area. The circle minimizes mean internal distance for a given area, so the index takes its lower bound of one for a perfectly circular footprint and rises as the footprint becomes elongated, lobed or fragmented; because the normalization removes area, the index captures shape alone and not city size. Higher values therefore mean that water and traffic must travel further, on average, between two points of the built-up area. Additionally, population is from the 2015 1% Population Sample Survey.

Rainfall–congestion estimation

This subsection estimates how much travel time a day of rain costs a city. It produces the bin coefficients plotted in Fig. 1a and reported in Extended Data Table 1, which are also the inputs to the annual time losses below, and the single per-millimeter coefficient carried into the projections.

The main specification lets the response vary with rainfall intensity:

$$\text{Congestion}_{c,d} = \sum_{b=2}^{14} \beta_b \, \text{PrepBin}_{c,d}^{(b)} + X_{c,d} + \mu_c + \tau_d + \sigma_{c,q} + \varepsilon_{c,d} \tag{1}$$

The unit of observation is a city-day. $\text{Congestion}_{c,d}$ is the Congestion Delay Index of city c on day d, so a coefficient of 0.01 means travel time rises by 1 percent of the free-flow duration. The day's precipitation is classified into fourteen exhaustive categories: dry days, twelve 2 mm bands from 0 to 24 mm, and a top category collecting days above 24 mm. Dry days are the omitted reference, so $\text{PrepBin}_{c,d}^{(b)}$ denotes the thirteen indicators for the remaining categories, indexed $b = 2, \ldots, 14$, and β_b is the travel-time cost of a day in band b relative to a dry day. $X_{c,d}$ denotes weather controls: daily mean temperature in 5°C bins between −20 and 30°C, with the end bins absorbing more extreme days and the bin containing 15°C omitted, together with daily mean wind speed and its square. The same $X_{c,d}$ enters equations (2), (3) and (4). The three fixed effects are city (μ_c),

calendar date (τ_d) and city-by-year-quarter ($\sigma_{c,q}$), so that β_b is identified from day-to-day variation within a city and a single quarter. Standard errors are clustered by city.

A linear counterpart replaces the bins with precipitation in millimeters, giving one coefficient β. Both are reported in Extended Data Table 1. The linear form is used in the projections, because projected rainfall is available only as a monthly total and carries no information about the distribution of daily intensities.

Annual time losses

This subsection converts the coefficients of equation (1) into hours, producing the city-level map in Fig. 1c and the national totals reported in the text. For city c, annual commuting time lost to rainfall is

$$L_c \;=\; 2 \times N_c \times T_c^{\mathrm{ff}} \times \sum_{b=2}^{14} \hat{\beta}_b^{\mathrm{wd}}\, D_{c,b}^{\mathrm{wd}} \tag{1a}$$

$\hat{\beta}_b^{\mathrm{wd}}$ are the weekday bin coefficients from column (3) of Extended Data Table 1, expressed as a fraction of free-flow travel time. $D_{c,b}^{\mathrm{wd}}$ counts the weekday days of the year on which city c recorded precipitation in band b, so the summation gives the fractional travel-time loss accumulated over a year. T_c^{ff} is the city's free-flow one-way commute duration in hours, constructed as described above. N_c is the number of residents commuting by car or bus, from the same survey. The factor of 2 converts a one-way trip into a round trip. L_c is therefore in person-hours per year, an aggregate over each city's commuting population.

Two conventions apply: only weekday rainy days are counted, at weekday coefficients, which lowers the total by about 15 percent relative to an all-days calculation; and every commuter is assumed to make two trips on a rainy day. Confidence intervals propagate the city-clustered covariance matrix of $\hat{\beta}^{\mathrm{wd}}$ through equation (1a). Equation (1a) is evaluated for the 98 estimation cities and, with the same coefficients, for all 289 cities with the required commuting and free-flow inputs; the 191 cities outside the estimation sample are out-of-sample predictions. Some figures have to be comparable with the interaction coefficient ρ, as in the equivalent time value of the Sponge City expansion. There the linear coefficient replaces the bin coefficients, which yields a smaller total for the same cities.

Infrastructure–precipitation interaction

Equation (1) imposes a common rainfall response on every city. This subsection asks whether that response depends on what a city has built, and produces the interaction coefficient ρ that underlies Fig. 2 and Extended Data Tables 3–6, as well as the drainage term carried into the projections. The rainfall coefficient is allowed to vary with infrastructure:

$$\mathrm{Congestion}_{c,d} = \beta\,\mathrm{Prep}_{c,d} + \rho\,\mathrm{Prep}_{c,d} \times \mathrm{Infra}_{c,y} + X_{c,d} + \mu_c + \tau_d + \sigma_{c,q} + \varepsilon_{c,d} \tag{2}$$

$\mathrm{Prep}_{c,d}$ is daily precipitation in millimeters. $\mathrm{Infra}_{c,y}$ is a city-year measure of infrastructure

density, assigned to every day of calendar year y; the yearbook reports year-end stocks. ρ is the object of interest: the amount by which one additional unit of infrastructure changes the travel time a city loses per millimeter of rain, so that $\beta + \rho$ Infra is the effective rainfall damage function. The infrastructure main effect is absorbed by the city and city-by-quarter fixed effects. The sample is the 135,009 city-days of the 98 cities with pipeline records after merging the congestion index with the yearbook's pipeline series.

Pipeline density is measured in km/km^2. Extended Data Tables 3, 4, 5, 6 and 8 standardize each measure over the estimation sample, pooling city-days (1 SD = 3.22 km/km^2 for rainwater pipelines), so that magnitudes are comparable across infrastructure types. The Sponge City event studies and the projections use km/km^2 directly. Marginal effects quoted in the main text are evaluated at the city-level mean and standard deviation across the 98 estimation cities (5.40 and 2.98 km/km^2), which differ from the pooled city-day standard deviation used for standardization.

The identifying assumption is not that pipeline density is exogenous, but that no omitted city characteristic simultaneously (i) varies at the city-year level, (ii) interacts with daily precipitation, and (iii) operates outside the drainage channel. Four checks bear on this assumption: three comparisons that should come out empty if the drainage reading is wrong, and one gradient that should strengthen with it. Entering the four underground pipe networks in the same regression, and comparing across transport infrastructure, tests (iii) directly. The visibility decomposition tests the shock side. The terrain and urban-form gradients provide positive evidence: terrain slope is geologically given and cannot be altered by urban policy, so the strengthening of pipeline buffering with slope cannot reflect reverse causality from drainage investment to the moderator; urban shape, though partly a policy outcome, is only weakly correlated with slope ($r = 0.20$), and each moderator reproduces the same gradient when entered on its own.

Visibility decomposition. Drainage removes water from the road but cannot improve visibility, so comparing the two channels tests whether the pipeline interaction is specific to surface water. Visibility is taken from GSOD station observations and converted from miles to kilometers, with the top code of 18.6 miles ($\approx$ 29.9 km) treated as right-censored. It enters continuously, in kilometers. Equation (2) is re-estimated on the fixed subsample with non-missing visibility (133,778 city-days), adding the visibility main effect and then its interaction with pipeline density. The change in the pipeline–precipitation coefficient is tested with a city-clustered bootstrap (999 replications) under the full fixed-effect structure ($\Delta\rho = 1.38 \times 10^{-5}$, 95% CI $[0.48, 2.28] \times 10^{-5}$), and equality of the standardized pipeline responses to precipitation and to low visibility is rejected at $p = 0.020$. A further check restricts attention to precipitation-free days, on which visibility varies independently of surface water; there its interaction with pipeline density is near zero.

Sponge City Program evaluation

This subsection asks whether the drainage margin responds to policy. It produces three sets of estimates: the rainfall–congestion slope difference between pilot and non-pilot cities; the effect of pilot designation on infrastructure stocks, shown as event studies in Fig. 3 and as static esti-

mates in Extended Data Table 7; and a specification that establishes the slope difference is driven by rainwater pipes rather than by other observed infrastructure pilot cities have (Extended Data Table 8).

The Sponge City Program was announced around the end of 2015 and directs central transfers to thirty pilot cities for stormwater capacity. We date treatment from 2016, when transfers were disbursed and construction began to register in the yearbook; the event-study coefficients are flat through 2015. The pilot cities are the treated group and all other cities in the panel are controls.

The rainfall–congestion slope is first allowed to differ by pilot status:

$$\text{Congestion}_{c,d} = \beta\,\text{Prep}_{c,d} + \theta\,\text{Prep}_{c,d} \times \text{Policy}_c + X_{c,d} + \mu_c + \tau_d + \sigma_{c,q} + \varepsilon_{c,d} \tag{3}$$

estimated on the same 141,493 city-days as equation (1). Policy_c is a time-invariant indicator for pilot status, so θ is the difference in travel-time cost per millimeter between pilot and non-pilot cities. The congestion series begins in October 2015 and is too short before treatment to test for parallel pre-trends, so we use the annual construction-yearbook panel to test the parallel trend assumption:

$$\text{Infra}_{c,y} = \sum_{k \neq 2015} \delta_k\,\text{Treat}_c \times \mathbf{1}[y = k] + X_{c,y} + \mu_c + \tau_y + \varepsilon_{c,y} \tag{3a}$$

The unit of observation is a city-year, 2011 to 2019, and the panel is unbalanced. $\text{Infra}_{c,y}$ is in turn rainwater pipeline density, sewer pipeline density, water-supply pipeline density and green land coverage. δ_k traces the pilot–control difference year by year, with 2015 omitted so that all coefficients are read relative to the year before treatment. $X_{c,y}$ denotes weather controls in this annual panel: annual mean daily temperature in six 5°C bins spanning 0 to 25°C, and annual mean daily precipitation in seven 1 mm bins spanning 0 to 6 mm, with the top bin collecting city-years above 6 mm. Fixed effects are city (μ_c) and year (τ_y); standard errors are clustered by city. The static difference-in-differences collapses the post-treatment indicators into $\text{Treat}_c \times \text{Post}_y$.

Equations (2) and (3) each relate rainfall sensitivity to one variable, and the two are correlated because the program expanded pipes. Entering both interactions together separates them:

$$\begin{aligned}\text{Congestion}_{c,d} = {} & \beta\,\text{Prep}_{c,d} + \theta\,\text{Prep}_{c,d} \times \text{Policy}_c + \rho\,\text{Prep}_{c,d} \times \text{Pipe}_{c,y} \\ & + \sum_j \gamma_j\,\text{Prep}_{c,d} \times \text{Infra}^j_{c,y} + X_{c,d} + \mu_c + \tau_d + \sigma_{c,q} + \varepsilon_{c,d}\end{aligned} \tag{4}$$

$\text{Infra}^j_{c,y}$ collects the other infrastructure groups—other pipe networks, transport infrastructure, and green coverage—each entered on its own in columns (2)–(4) of Extended Data Table 8 with ρ excluded, and all together with ρ in column (6). Column (5) sets every γ_j to zero and is the specification discussed in the main text. If the flatter slope of pilot cities operates through the pipes the program laid, then conditioning on pipeline density should absorb θ while leaving ρ intact. That is what happens: θ halves and loses significance, while ρ retains 87 percent of its magnitude from equation (2). The pilot indicator, in other words, carries little information about

rainfall sensitivity once drainage is measured directly.

Instrumental variables. As a further check, we instrument the pipeline–precipitation interaction with the pilot indicator interacted with precipitation, estimating by LIML. The first stage is weak (Kleibergen–Paap $F = 4.5$), so inference relies on weak-identification-robust statistics, which are marginal (Anderson–Rubin $p = 0.093$; Stock–Wright $p = 0.081$). The IV point estimate is larger than OLS by a factor of 1.7 and of the same sign (-0.648 against -0.378 on the standardized scale), consistent with attenuation bias. The IV is treated as complementary evidence, and all projections use OLS estimates.

Climate projections

This subsection asks how much additional drainage each city would need to hold its congestion exposure constant as rainfall changes, producing the gaps mapped in Fig. 4c–e. We call that quantity the city's drainage gap, Gap_c, measured in km/km^2 of additional rainwater pipeline. It is a function of two city characteristics and the estimated parameters,

$$\underbrace{\text{Gap}_c}_{\text{drainage gap}} = f\left(\underbrace{\text{Pipe}_c}_{\substack{\text{existing}\\ \text{stock}}},\ \underbrace{\Delta P_c,\ P_c^{\text{fut}}}_{\substack{\text{projected}\\ \text{rainfall}}};\ \underbrace{\beta,\ \rho}_{\substack{\text{estimated}\\ \text{coefficients}}}\right)$$

increasing in the rainfall a city will face and decreasing in the drainage it already has.

Annual congestion exposure under the linear specification is the effective slope times annual rainfall, $(\beta + \rho\,\text{Pipe}_c)\,P_c$. The gap is defined as the additional density that would hold that exposure at its current level once rainfall reaches P_c^{fut}:

$$\underbrace{(\beta + \rho\,\text{Pipe}_c)\,P_c}_{\text{exposure today}} = \underbrace{\left(\beta + \rho\,(\text{Pipe}_c + \text{Gap}_c)\right)\,P_c^{\text{fut}}}_{\text{exposure at mid-century, with the gap closed}}$$

Expanding the right-hand side and collecting the terms in Gap_c gives $\rho\,\text{Gap}_c\,P_c^{\text{fut}} = (\beta + \rho\,\text{Pipe}_c)\,(P_c - P_c^{\text{fut}})$, and since $P_c - P_c^{\text{fut}} = -\Delta P_c$, dividing through by $\rho\,P_c^{\text{fut}}$ yields the closed form

$$\text{Gap}_c = -\,\frac{(\beta + \rho\,\text{Pipe}_c)\,\Delta P_c}{\rho\,P_c^{\text{fut}}} \tag{5}$$

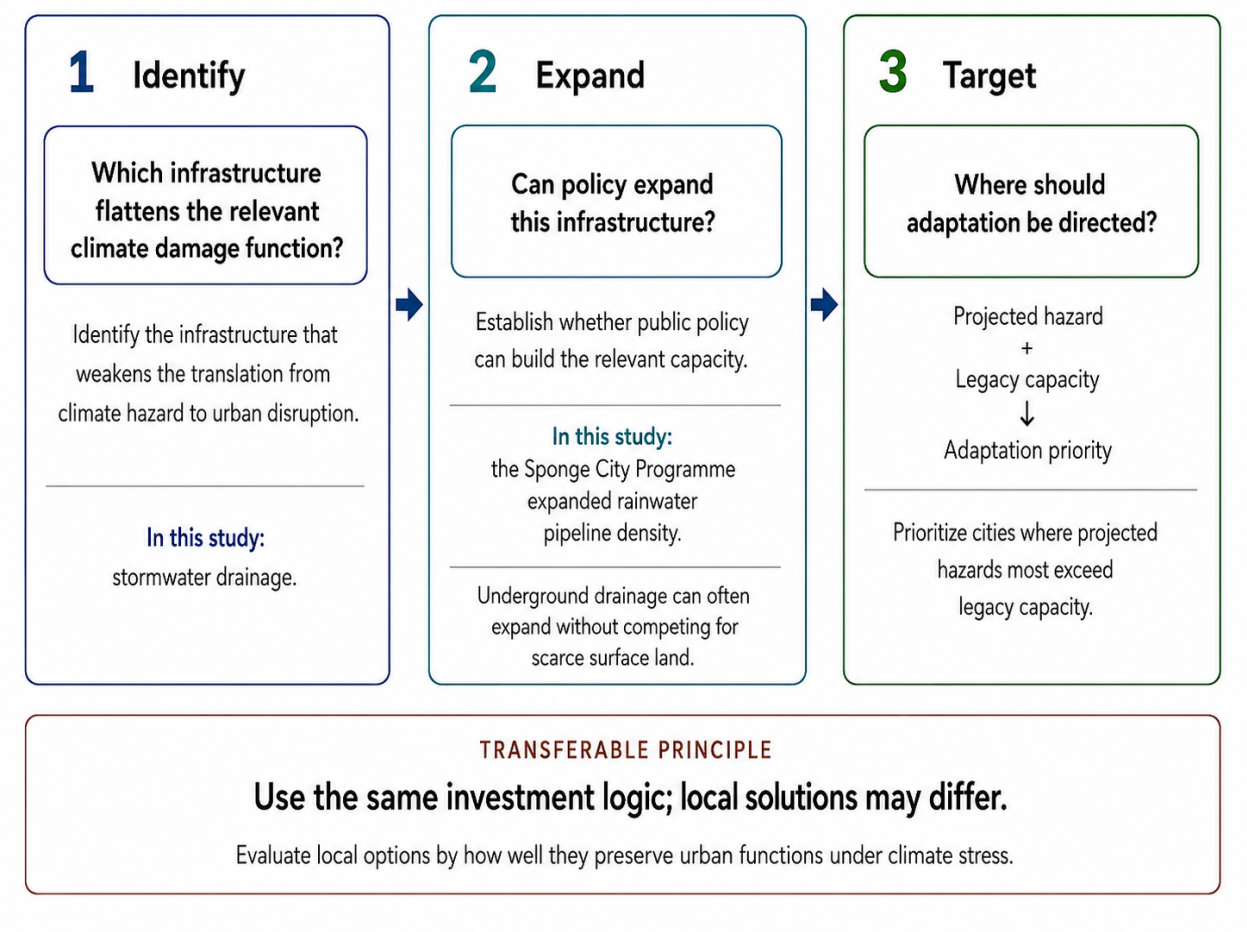
Equation (5) has four inputs. $\beta = 3.199 \times 10^{-3}$ (s.e. 2.77×10^{-4}) per mm and $\rho = -1.175 \times 10^{-4}$ (s.e. 3.70×10^{-5}) per mm per km/km^2. We use OLS rather than IV, and the linear rather than the bin specification, because projected precipitation is resolved only to monthly totals and carries no information about the distribution of daily intensities. Pipe_c is the city's 2019 rainwater pipeline density. P_c^{fut} is annual precipitation in 2041–2050 and ΔP_c its increase over 2021–2030, both from the CMIP6 product described above: each city is matched to the 1-km grid cells within its administrative boundary, monthly precipitation is averaged over those cells and summed to

annual totals, and the two windows are differenced within each model before averaging across the three. Multiplying Gap_c by built-up area converts the density into kilometers of pipe.

Only P_c^{fut} and ΔP_c are scenario-specific, so gaps differ across scenarios through projected rainfall alone. Across the 342 matched cities the population-weighted increase in annual precipitation is 10.0 percent under SSP119, 4.8 percent under SSP245 and 6.3 percent under SSP585. The effective slope $\beta + \rho\,\text{Pipe}$ reaches zero at 27.2 km/km^2, above the range spanned by the estimation sample.

Equation (5) is evaluated for every city with an infrastructure record; the 99-city congestion sample is used for estimation only. Of the 342 cities matched to the CMIP6 projections, 324 also have a 2019 pipeline record and 301 of those also report built-up area. Cities with $\Delta P_c \leq 0$ enter with a gap of zero, and cities with rising rainfall but no built-up area record are absent from the totals, which are accordingly lower bounds. The calculation holds population, behavior, built-up area, the 2019 pipeline stock and non-drainage infrastructure fixed, and applies a single ρ to every city.

Extended Data



Extended Data Fig. 1 | A three-step framework for climate-resilience investment. The framework asks, in order, which infrastructure flattens the relevant climate damage function, whether public policy can expand that infrastructure, and where the resulting capacity should be directed. **Step 1, Identify:** find the infrastructure that weakens the translation from climate hazard to the loss of an urban function; here, stormwater drainage for rainfall and road mobility. **Step 2, Expand:** establish whether public policy can build the relevant capacity; here, the Sponge City Program expanded rainwater pipeline density, and underground drainage could do so without competing for scarce surface land. **Step 3, Target:** combine projected hazard with legacy capacity to set adaptation priority, directing investment to the cities where projected hazards most exceed the network already in place. The logic is transferable even where the answer is not: cities elsewhere should evaluate locally appropriate options by how well each preserves urban functions under climate stress, rather than replicating a particular drainage standard.

Extended Data Table 1 | Effects of Precipitation on Urban Congestion

	Congestion Index				
Precipitation	(1)	(2)	(3) Weekday	(4) Weekend	(5) Linear
0–2 mm	0.010***	0.010***	0.012***	0.005***	
	(0.002)	(0.001)	(0.002)	(0.001)	
2–4 mm	0.038***	0.035***	0.041***	0.019***	
	(0.004)	(0.003)	(0.004)	(0.002)	
4–6 mm	0.050***	0.048***	0.058***	0.022***	
	(0.004)	(0.003)	(0.004)	(0.003)	
6–8 mm	0.055***	0.051***	0.061***	0.027***	
	(0.004)	(0.004)	(0.004)	(0.003)	
8–10 mm	0.061***	0.058***	0.071***	0.025***	
	(0.004)	(0.004)	(0.004)	(0.003)	
10–12 mm	0.069***	0.067***	0.080***	0.036***	
	(0.004)	(0.004)	(0.005)	(0.003)	
12–14 mm	0.075***	0.071***	0.085***	0.036***	
	(0.004)	(0.004)	(0.005)	(0.004)	
14–16 mm	0.081***	0.078***	0.090***	0.036***	
	(0.005)	(0.005)	(0.006)	(0.005)	
16–18 mm	0.081***	0.077***	0.095***	0.031***	
	(0.006)	(0.006)	(0.007)	(0.005)	
18–20 mm	0.087***	0.083***	0.106***	0.028***	
	(0.007)	(0.006)	(0.007)	(0.005)	
20–22 mm	0.082***	0.078***	0.095***	0.039***	
	(0.006)	(0.006)	(0.007)	(0.006)	
22–24 mm	0.094***	0.091***	0.111***	0.046***	
	(0.008)	(0.007)	(0.009)	(0.009)	
>24 mm	0.109***	0.107***	0.132***	0.041***	
	(0.005)	(0.005)	(0.006)	(0.004)	
Per mm (linear)					0.002***
					(0.000)
Weather controls	No	Yes	Yes	Yes	Yes
City FE	Yes	Yes	Yes	Yes	Yes
Date FE	Yes	Yes	Yes	Yes	Yes
City × Quarter FE	No	Yes	Yes	Yes	Yes
Observations	141,493	141,493	101,021	40,472	141,493

Note: Effect of a day's rainfall on the congestion index, by intensity, from equation (1). Observations are city-days; dry days are the omitted reference; standard errors, clustered by city, in parentheses.

The estimation sample is 141,493 city-days: 99 cities from October 2015 to December 2019, out of 153,648 potential city-days, with 12,155 dropped because the congestion index is missing. No observation is lost to missing weather.

Columns (1)–(4) report the bin specification and column (5) the linear one, whose per-millimeter coefficient is not comparable in scale. Columns (3)–(4) restrict the sample to weekdays and weekends; column (3) supplies the coefficients used for the annual time losses and column (5) the one used in the projections.

*** $p < 0.01$, ** $p < 0.05$, * $p < 0.1$.

Extended Data Table 2 | Dynamic Effects of Precipitation on Urban Congestion

	Congestion Index	
Precipitation on day	(1)	(2)
$d-7$	0.0001^{**} (0.0000)	0.0001^{**} (0.0000)
$d-6$	0.0001^{***} (0.0000)	0.0001^{***} (0.0000)
$d-5$	0.0001^{*} (0.0000)	0.0001^{*} (0.0000)
$d-4$	0.0001^{***} (0.0000)	0.0001^{***} (0.0000)
$d-3$	0.0002^{***} (0.0000)	0.0002^{***} (0.0000)
$d-2$	0.0002^{***} (0.0000)	0.0002^{***} (0.0000)
$d-1$	-0.0001^{***} (0.0000)	-0.0001^{***} (0.0000)
d **(day of rainfall)**	$\mathbf{0.0023}^{***}$ (0.0002)	$\mathbf{0.0023}^{***}$ (0.0002)
$d+1$	0.0005^{***} (0.0000)	0.0005^{***} (0.0000)
$d+2$	-0.0000 (0.0000)	-0.0000 (0.0000)
$d+3$	-0.0000 (0.0000)	-0.0000 (0.0000)
$d+4$	-0.0000 (0.0000)	-0.0000 (0.0000)
$d+5$	0.0000 (0.0000)	0.0000 (0.0000)
$d+6$	-0.0000 (0.0000)	-0.0000 (0.0000)
$d+7$	-0.0000 (0.0000)	-0.0000 (0.0000)
Weather controls	No	Yes
City FE	Yes	Yes
Date FE	Yes	Yes
City $\times$ Quarter FE	No	Yes
Observations	140,478	140,478

Note: Response of congestion to precipitation on the surrounding fourteen days, from a single regression of the linear form of equation (1) including seven lags and seven leads. Row $d-k$ is rainfall k days earlier and $d+k$ k days later; leads serve as a placebo. Observations are city-days; standard errors, clustered by city, in parentheses. The seven-day window drops observations at the ends of each city's series.
Column (1) omits weather controls and city-by-quarter fixed effects. The same coefficients are plotted in Fig. 1b.
*** $p<0.01$, ** $p<0.05$, * $p<0.1$.

Extended Data Table 3 | Underground Pipe Networks and Rainfall Buffering

	Congestion Index				
	(1)	(2)	(3)	(4)	(5)
Rainwater × Prcp	-0.378^{***}				-0.411^{**}
	(0.119)				(0.174)
Sewage × Prcp		-0.239			$+0.085$
		(0.157)			(0.135)
Water supply × Prcp			-0.251^{*}		-0.161
			(0.147)		(0.159)
Gas × Prcp				-0.007	$+0.186$
				(0.165)	(0.150)
Prcp	2.558^{***}	2.494^{***}	2.531^{***}	2.452^{***}	2.612^{***}
	(0.155)	(0.164)	(0.171)	(0.186)	(0.158)
Weather controls	Yes	Yes	Yes	Yes	Yes
City FE	Yes	Yes	Yes	Yes	Yes
Date FE	Yes	Yes	Yes	Yes	Yes
City × Quarter FE	Yes	Yes	Yes	Yes	Yes
Observations	135,009	135,009	135,009	135,009	135,009

Note: Rainfall buffering by each of the four buried pipe networks, from equation (2). Coefficients $\times 10^{-3}$; pipe densities standardized to unit variance; observations are city-days; standard errors, clustered by city, in parentheses. The precipitation coefficient is evaluated at mean pipeline density. Lhasa has no pipeline record in the yearbook and is dropped, leaving 98 of the 99 congestion cities.

Columns (1)–(4) enter one network at a time and column (5) all four together; a blank cell means the network is not included in that regression.

In column (5), tests of equality with the rainwater coefficient give sewage $F = 3.15$ ($p = 0.079$), water supply $F = 0.73$ ($p = 0.395$) and gas $F = 12.77$ ($p = 0.001$).

*** $p < 0.01$, ** $p < 0.05$, * $p < 0.1$.

Extended Data Table 4 | Infrastructure Comparison: Rainfall Attenuation by Type

Infrastructure × Prcp	(1) One at a time	(2) All entered together
Stormwater-related		
Rainwater pipeline density	-0.378^{***} (0.119)	-0.400^{**} (0.172)
Green land coverage	-0.363^{***} (0.136)	-0.238^{**} (0.108)
Other underground pipe networks		
Sewage pipeline density	-0.239 (0.157)	$+0.088$ (0.127)
Water-supply pipeline density	-0.251^{*} (0.147)	-0.053 (0.152)
Gas pipeline density	-0.007 (0.165)	$+0.126$ (0.148)
Transport and street infrastructure		
Bus fleet	-0.220 (0.159)	-0.115 (0.155)
Taxi fleet	-0.133 (0.264)	$+0.084$ (0.216)
Road width	$+0.047$ (0.166)	$+0.109$ (0.150)
Streetlights	-0.111 (0.153)	$+0.005$ (0.149)
Subway length	$+0.009$ (0.252)	—
Prcp	2.449–2.558^{***}	2.672^{***} (0.159)
Weather controls	Yes	Yes
City FE	Yes	Yes
Date FE	Yes	Yes
City × Quarter FE	Yes	Yes
Observations	135,009	135,009

Note: Rainfall buffering by type of urban infrastructure, from equation (2) with the listed measure in place of pipeline density. Coefficients $\times 10^{-3}$; all measures standardized to unit variance; observations are city-days; standard errors, clustered by city, in parentheses.

Column (1) is one regression per row, so the precipitation coefficient differs across rows and its range is given; column (2) is a single regression entering all interactions together.

Subway length is observed for a minority of cities, so its row in column (1) rests on 45,551 city-days with a precipitation coefficient of 3.207; the range in column (1) covers the nine measures estimated on the full sample. It is excluded from column (2) because it measures a substitute travel mode rather than a capacity to shed water.

*** $p < 0.01$, ** $p < 0.05$, * $p < 0.1$.

Extended Data Table 5 | Rainwater Pipelines, Precipitation, and Visibility

	Congestion Index		
	(1) Baseline, common sample	(2) + Visibility	(3) Full channel
Pipe × Prcp	-0.392^{***}	-0.378^{***}	-0.376^{***}
	(0.118)	(0.117)	(0.116)
Pipe × Visibility	—	—	$+0.037$
			(0.127)
Visibility main effect	No	Yes	Yes
Weather controls	Yes	Yes	Yes
City / Date / City × Quarter FE	Yes	Yes	Yes
Observations	133,778	133,778	133,778

Note: Whether rainwater pipelines buffer poor visibility as well as rainfall, from equation (2) estimated on the subsample with non-missing visibility, adding the visibility main effect in column (2) and its interaction with pipeline density in column (3). Coefficients $\times 10^{-3}$; pipeline density standardized (1 SD = 3.22 km/km^2); precipitation in mm and visibility in km, so higher values mean clearer conditions. Observations are city-days; standard errors, clustered by city, in parentheses. A dash marks a term not included in that regression.

Visibility enters continuously throughout this table. Column (1) re-estimates the baseline on this subsample; its coefficient differs from the full-sample estimate in Extended Data Table 3 only through the change in sample.

*** $p < 0.01$, ** $p < 0.05$, * $p < 0.1$.

Extended Data Table 6 | Terrain, Urban Form, and Pipeline Buffering

	Congestion Index		
Moderator entered:	(1) Slope	(2) Shape	(3) Both
Panel A: Buffering as a continuous function of the moderator			
Prcp × Pipe	-0.338^{***} (0.116)	-0.238^{**} (0.100)	-0.229^{**} (0.106)
Prcp × Slope	0.4^{*} (0.3)	—	0.1 (0.3)
Prcp × Pipe × Slope	-0.248^{**} (0.109)	—	-0.029 (0.116)
Prcp × Shape	—	0.47^{*} (0.24)	0.5^{*} (0.3)
Prcp × Pipe × Shape	—	-0.403^{***} (0.113)	-0.409^{***} (0.135)
Observations	135,009	135,009	135,009
Panel B: Buffering re-estimated separately within terciles of the moderator			
	Tercile 1	Tercile 2	Tercile 3
Terciles of terrain slope			
Median slope (°)	3.65	7.13	11.98
Prcp × Pipe	-0.048 (0.127)	-0.248^{**} (0.122)	-0.464 (0.283)
Observations	45,370	44,174	45,465
Terciles of shape irregularity			
Median index	1.11	1.22	1.35
Prcp × Pipe	0.071 (0.250)	-0.187 (0.122)	-0.766^{***} (0.230)
Observations	48,296	44,919	41,794
Weather controls	Yes	Yes	Yes
City / Date / City × Quarter FE	Yes	Yes	Yes

Note: Where pipeline buffering is strongest, from equation (2) augmented with a moderator and its interactions. Coefficients $\times 10^{-3}$; pipeline density, slope and shape are all standardized to unit variance (1 SD = 3.22 km/km^2 for pipeline density), so a moderator value of zero is the sample mean and one unit is one standard deviation. Observations are city-days; standard errors, clustered by city, in parentheses. A dash marks a term not included in that regression.

How to read Panel A. The buffering of a city whose moderator takes value m is the *Prcp* × *Pipe* coefficient plus m times the triple interaction. In column (1), for instance, pipelines flatten the rainfall slope by 0.338 at the average terrain slope and by a further 0.248 for each standard deviation of additional slope. More negative means more buffering.

Columns (1) and (2) enter one moderator at a time and column (3) both together, where the two triple interactions are highly correlated. Panel B splits the sample by tercile instead of imposing a functional form.

*** $p < 0.01$, ** $p < 0.05$, * $p < 0.1$.

Extended Data Table 7 | Effects of Sponge City on Infrastructure

Panel A: Effect on each infrastructure stock

	Rain pipe	Sewer pipe	Green	Water supply
Treat × Post	1.252**	0.097	0.001	0.311
	(0.542)	(0.341)	(0.006)	(0.775)
Mean	3.406	3.904	0.346	12.09
Observations	4,552	4,552	4,552	4,552
Weather controls	Yes	Yes	Yes	Yes
City / Year FE	Yes	Yes	Yes	Yes

Panel B: Robustness of the rainwater pipeline effect

	(1) Base	(2) Length	(3) 99 Cities	(4) Prov×Yr	(5) Extra	(6) Prefect.
Treat × Post	1.252**	705.6***	1.003	1.531**	1.548**	1.126**
	(0.542)	(170.7)	(0.610)	(0.626)	(0.649)	(0.511)
Observations	4,552	4,552	866	4,503	4,503	2,408
Weather controls	Yes	Yes	Yes	Yes	Yes	Yes
City / Year FE	Yes	Yes	Yes	Yes	Yes	Yes

Note: Effect of Sponge City designation on infrastructure stocks, from the static form of equation (3a), $\text{Treat}_c \times \text{Post}_y$. Observations are city-years, 2011–2019, on the unbalanced construction-yearbook panel; standard errors, clustered by city, in parentheses. *Mean* is the sample mean of the dependent variable. Weather controls are annual mean daily temperature and precipitation bins (see Methods).

Panel A reports one regression per outcome. Rainwater, sewer and water-supply pipelines are measured in km/km^2 and green land coverage as a share of built-up area.

Panel B keeps rainwater pipeline density as the outcome and varies the specification. Col (1) repeats the Panel A baseline. Col (2) uses total pipeline length in km rather than density, which puts its coefficient on a different scale. Col (3) restricts the sample to the 99 congestion cities. Col (4) adds province-by-year fixed effects. Col (5) additionally interacts six pre-program (2011) city characteristics—GDP per capita, subway-line density, road width, streetlight density, and taxi and bus fleets per capita—with linear year trends. Col (6) restricts to prefecture-level cities.

*** $p < 0.01$, ** $p < 0.05$, * $p < 0.1$.

Extended Data Table 8 | Sponge City, Pipelines, and Rainfall Sensitivity

	Congestion Index					
	(1)	(2)	(3)	(4)	(5)	(6)
SpongeCity × Prcp	-0.725^{*}	-0.629^{*}	-0.658^{**}	-0.637^{*}	-0.373	-0.351
	(0.407)	(0.348)	(0.329)	(0.371)	(0.294)	(0.292)
Pipe_{std} × Prcp					-0.329^{***}	-0.352^{**}
					(0.108)	(0.174)
Precipitation interacted with:						
Other pipe networks	No	Yes	No	No	No	Yes
Transport infrastructure	No	No	Yes	No	No	Yes
Green coverage	No	No	No	Yes	No	Yes
Rainwater pipelines	No	No	No	No	Yes	Yes
Weather controls	Yes	Yes	Yes	Yes	Yes	Yes
City / Date / City × Quarter FE	Yes	Yes	Yes	Yes	Yes	Yes
Observations	135,009	135,009	135,009	135,009	135,009	135,009

Note: Whether the flatter rainfall–congestion slope of pilot cities operates through the pipes the program laid. Column (1) estimates equation (3). Columns (2)–(4) each add the precipitation interactions of one group of other infrastructure, entered on its own; column (5) adds the rainwater pipeline interaction instead and is the specification discussed in the main text. Column (6) enters all four groups together and is therefore not the sum of the preceding columns.

Other pipe networks are sewage, water supply and gas; *transport infrastructure* is bus fleet, taxi fleet, road width and street lighting. Coefficients on these interactions are reported in Extended Data Table 4.

All columns use the 98 cities with pipeline records so that the estimates share common observations.

*** $p < 0.01$, ** $p < 0.05$, * $p < 0.1$.

Extended Data Table 9 | OLS vs. IV Estimates

	OLS	IV
β (Prcp)	2.56^{***}	2.63^{***}
	(0.15)	(0.19)
ρ (Pipe $\times$ Prcp)	-0.378^{***}	-0.648^{**}
	(0.119)	(0.263)
Weather controls	Yes	Yes
City / Date / City $\times$ Quarter FE	Yes	Yes
Observations	135,009	135,009
KP F		4.50
AR p		0.093
SW p		0.081

Note: Instrumental-variables check on the pipeline interaction. Column (1) estimates equation (2) by OLS; column (2) instruments the pipeline–precipitation interaction with the pilot indicator interacted with precipitation and estimates by LIML. Coefficients $\times 10^{-3}$; pipeline density standardized (1 SD = 3.22 km/km^2), so β is evaluated at mean pipeline density. Observations are city-days; standard errors, clustered by city, in parentheses.

KP F is the Kleibergen–Paap first-stage statistic, for which a conventional threshold is 10; at 4.50 it indicates a weak first stage. AR and SW are the Anderson–Rubin and Stock–Wright tests, which remain valid under weak identification; both reject at the 10 percent but not the 5 percent level.

Stars in the IV column are based on conventional standard errors and are not valid under a weak first stage; inference on the IV estimate should be read from the AR and SW statistics.

*** $p < 0.01$, ** $p < 0.05$, * $p < 0.1$.

References

[1] Elmqvist, T. *et al.* Sustainability and resilience for transformation in the urban century. *Nature Sustainability* **2**, 267–273 (2019).

[2] Akbar, P. A., Couture, V., Duranton, G. & Storeygard, A. The fast, the slow, and the congested: Urban transportation in rich and poor countries. NBER Working Paper 31642, National Bureau of Economic Research (2023).

[3] Seneviratne, S. I. *et al.* Weather and climate extreme events in a changing climate. In Masson-Delmotte, V. *et al.* (eds.) *Climate Change 2021: The Physical Science Basis. Contribution of Working Group I to the Sixth Assessment Report of the Intergovernmental Panel on Climate Change*, chap. 11, 1513–1766 (Cambridge University Press, Cambridge, UK and New York, NY, USA, 2021).

[4] Couture, V., Duranton, G. & Turner, M. A. Speed. *The Review of Economics and Statistics* **100**, 725–739 (2018).

[5] He, Y., Thies, S., Avner, P. & Rentschler, J. Flood impacts on urban transit and accessibility—a case study of kinshasa. *Transportation Research Part D: Transport and Environment* **96**, 102889 (2021).

[6] He, C. *et al.* The overlooked health impacts of extreme rainfall exposure in 30 East Asian cities. *Nature Sustainability* **7**, 423–431 (2024).

[7] Duranton, G. & Turner, M. A. The fundamental law of road congestion: Evidence from US cities. *American Economic Review* **101**, 2616–2652 (2011).

[8] Chan, F. K. S., Chen, W. Y., Gu, X., Peng, Y. & Sang, Y. Transformation towards resilient sponge cities in China. *Nature Reviews Earth & Environment* **3**, 99–101 (2022).

[9] Kong, F., Sun, S. & Lei, T. Understanding China's urban rainstorm waterlogging and its potential governance. *Water* **13**, 891 (2021).

[10] Wilcox, L. J. *et al.* Accelerated increases in global and Asian summer monsoon precipitation from future aerosol reductions. *Atmospheric Chemistry and Physics* **20**, 11955–11977 (2020).

[11] Belloc, I., Giménez-Nadal, J. I. & Molina, J. A. Weather conditions and daily commuting. *Journal of Regional Science* **65**, 818–842 (2025).

[12] Dell, M., Jones, B. F. & Olken, B. A. What do we learn from the weather? The new climate-economy literature. *Journal of Economic Literature* **52**, 740–798 (2014).

[13] General Office of the State Council of the People's Republic of China. Guiding opinions on promoting the construction of sponge cities (Guo Ban Fa [2015] no. 75). State Council of the People's Republic of China (2015). URL https://www.gov.cn/zhengce/content/2015-10/16/content_10228.htm. In Chinese.

[14] Koks, E. E. *et al.* A global multi-hazard risk analysis of road and railway infrastructure assets. *Nature Communications* **10**, 2677 (2019).

[15] Hallegatte, S., Rentschler, J. & Rozenberg, J. *Lifelines: The Resilient Infrastructure Opportunity* (World Bank, Washington, DC, 2019).

[16] Tellman, B. *et al.* Satellite imaging reveals increased proportion of population exposed to floods. *Nature* **596**, 80–86 (2021).

[17] Rentschler, J. *et al.* Global evidence of rapid urban growth in flood zones since 1985. *Nature* **622**, 87–92 (2023).

[18] Liu, H. & Bai, X. Intercity connectivity enhances urban mobility resilience to extreme rainfall. *Nature Climate Change* **16**, 1037–1044 (2026).

[19] Li, C. *et al.* Adaptive capacity for multimodal transport network resilience to extreme floods. *Nature Sustainability* **8**, 741–752 (2025).

[20] Tanoue, M., Taguchi, R., Alifu, H. & Hirabayashi, Y. Residual flood damage under intensive adaptation. *Nature Climate Change* **11**, 823–826 (2021).

[21] Aerts, J. C. J. H. *et al.* Exploring the limits and gaps of flood adaptation. *Nature Water* **2**, 719–728 (2024).

[22] Akbar, P. A., Couture, V., Duranton, G. & Storeygard, A. Mobility and congestion in urban India. *American Economic Review* **113**, 1083–1111 (2023).

[23] Anderson, M. L. Subways, strikes, and slowdowns: The impacts of public transit on traffic congestion. *American Economic Review* **104**, 2763–2796 (2014).

[24] Gu, Y., Jiang, C., Zhang, J. & Zou, B. Subways and road congestion. *American Economic Journal: Applied Economics* **13**, 83–115 (2021).

[25] Alsan, M. & Goldin, C. Watersheds in child mortality: The role of effective water and sewerage infrastructure, 1880–1920. *Journal of Political Economy* **127**, 586–638 (2019).

[26] Cutler, D. & Miller, G. The role of public health improvements in health advances: The twentieth-century United States. *Demography* **42**, 1–22 (2005).

[27] Zhang, L. *et al.* Reduced flood-related bacillary dysentery risk with sponge city development in China. *Nature Cities* (2026).

[28] Kouassi, R. Water-proofed: Floods and water infrastructure quality in the united states (2024). URL https://regiskouassi.github.io/research. Working paper, Université de Montréal.

[29] Ward, P. J. *et al.* A global framework for future costs and benefits of river-flood protection in urban areas. *Nature Climate Change* **7**, 642–646 (2017).

[30] Dottori, F., Mentaschi, L., Bianchi, A., Alfieri, L. & Feyen, L. Cost-effective adaptation strategies to rising river flood risk in Europe. *Nature Climate Change* **13**, 196–202 (2023).

[31] McCulloch, S. E., Schaelling, M. P., Turner, M. & Kitagawa, T. Sewers and urbanization in the developing world. NBER Working Paper 33597, National Bureau of Economic Research (2025). Revised December 2025.

[32] Kotz, M., Levermann, A. & Wenz, L. The effect of rainfall changes on economic production. *Nature* **601**, 223–227 (2022).

[33] Chen, X., Lin, Y. & Zhu, P. The impact of rainfall on productivity: Implications for Chinese manufacturing. *Journal of Comparative Economics* **53**, 389–411 (2025).

[34] Yang, J., Chen, S., Qin, P., Lu, F. & Liu, A. A. The effect of subway expansions on vehicle congestion: Evidence from Beijing. *Journal of Environmental Economics and Management* **88**, 114–133 (2018).

[35] Balboni, C. In harm's way? infrastructure investments and the persistence of coastal cities. *American Economic Review* **115**, 77–116 (2025).

[36] New York City Mayor's Office of Climate and Environmental Justice. Climate resiliency design guidelines, version 4.1. New York City (2022). URL https://www.nyc.gov/assets/sustainability/downloads/pdf/publications/CRDG-4-1-May-2022.pdf.

[37] Skougaard Kaspersen, P., Høegh Ravn, N., Arnbjerg-Nielsen, K., Madsen, H. & Drews, M. Comparison of the impacts of urban development and climate change on exposing european cities to pluvial flooding. *Hydrology and Earth System Sciences* **21**, 4131–4147 (2017).

[38] Fan, J. *et al.* Exploring how economic level drives urban flood risk. *Nature Communications* **16**, 4857 (2025).

[39] Peng, S. 1 km multi-scenario and multi-model monthly precipitation data for china in 2021–2100 (2022).

[40] Peng, S., Ding, Y., Liu, W. & Li, Z. 1 km monthly temperature and precipitation dataset for China from 1901 to 2017. *Earth System Science Data* **11**, 1931–1946 (2019).

[41] Farr, T. G. *et al.* The Shuttle Radar Topography Mission. *Reviews of Geophysics* **45**, RG2004 (2007).